

Superexchange in dilute magnetic dielectrics: Application to (Ti,Co)O₂

K. Kikoin

Department of Physics, Ben-Gurion University, Beer Sheva 84105, Israel

V. Fleurov*

*Raymond and Beverly Sackler Faculty of Exact Sciences, School of Physics and Astronomy, Tel-Aviv University, Tel-Aviv 69978 Israel
and Laue-Langevin Institute, F-38042, Grenoble, France*

(Received 16 May 2006; revised manuscript received 30 August 2006; published 7 November 2006)

We extend the model of ferromagnetic superexchange in dilute magnetic semiconductors to the ferromagnetically ordered highly insulating compounds (dilute magnetic dielectrics). The intrinsic ferromagnetism without free carriers is observed in oxygen-deficient films of anatase TiO₂ doped with transition-metal impurities in cation sublattice. We suppose that ferromagnetic order arises due to superexchange between complexes (oxygen vacancies + magnetic impurities), which are stabilized by charge transfer from vacancies to impurities. The Hund rule controls the superexchange via empty vacancy related levels so that it becomes possible only for the parallel orientation of impurity magnetic moments. The percolation threshold for magnetic ordering is determined by the radius of vacancy levels, but the exchange mechanism does not require free carriers. The crucial role of the nonstoichiometry in formation of the ferromagnetism makes the Curie temperatures extremely sensitive to the methods of sample preparation.

DOI: [10.1103/PhysRevB.74.174407](https://doi.org/10.1103/PhysRevB.74.174407)

PACS number(s): 75.50.Dd, 75.30.Et, 71.55.-i, 61.72.Ji

I. INTRODUCTORY NOTES

Recent experimental and theoretical investigations of dilute ferromagnetic semiconductors are concentrated mostly on II-VI and III-V materials doped with Mn impurities (see, e.g., Ref. 1). The theoretical explanation is based on the Vonsovskii-Zener model, which implies existence of a direct exchange interaction between the localized spins of magnetic ions (Mn) and itinerant spins of free carriers [holes in case of (Ga,Mn)As and related materials].² This interaction generates Ruderman-Kittel-Kasuya-Yosida (RKKY)-type indirect exchange between Mn ions, and the latter is claimed to be the source of long-range ferromagnetic (FM) order in dilute magnetic semiconductor (DMS) alloys. It was shown recently that the kinematic exchange interaction (specific version of superexchange between localized Mn moments via empty valence states of the host material) arises in *p*-type III-V DMS.³ This mechanism works together with the RKKY interaction because of the noticeable hybridization between *d* electrons of Mn ions and *p* holes near the top of the valence band. Both mechanisms are characterized by a direct proportionality between the carrier concentration and Curie temperature T_C . However, it was pointed out recently⁴ that an application of the RKKY based model to disordered DMS may be questionable if one properly takes oscillating character of the RKKY interaction into account.

Meanwhile, another family of dilute ferromagnetic alloys was discovered during the recent five years, where the ferromagnetic order with a high T_C exists in spite of the low carrier concentration. The ferromagnetic order was observed even in the insulating materials with carriers frozen out at $T \rightarrow 0$. These are metal oxides doped with transition-metal ions (see, e.g., Ref. 5 for a review). The absence of free carriers leaves no room for a RKKY interaction in this case, so the question about the origin of ferromagnetism arises anew.

The metal oxides like ZnO, SnO₂, TiO₂ are classified as wide-gap semiconductors. In this sense they are close to the wide-gap III-V nitrides GaN and AlN. We analyzed the case of *n*-(Ga,Mn)N in Ref. 3, where the leading interaction mechanism is the Zener-type double exchange⁶ via empty states in the impurity band. Magnetic ions (MIs) in all these compounds substitute for metallic cations. From this point of view, the difference between the two groups is in the charge state of substitutional impurity: the neutral state of an impurity should be MI³⁺ in nitrides and MI⁴⁺ in oxides. This difference implies different structures of spin multiplets, which is important for the magnetic properties of metallic alloys. However, due to a noticeable covalency of the host materials, MIs should saturate the broken bonds by its own valent electrons, which are donated by the 3*d* shells. This means that the violation of the electronic structure inserted by the dopants cannot be ignored in the studies of magnetic properties of DMSs.

Among the most salient features of magnetism in dilute ferromagnetic oxides one should mention an extreme sensitivity of the magnetic order to the growth and annealing conditions.^{5,7} We believe that this is an integral feature of magnetism in these materials, and the ferromagnetic ordering with high T_C is mediated by intrinsic or extrinsic defects, which form complexes with magnetic dopants. Such point of view is supported by recent experimental studies of Co-doped⁸ and Cr-doped⁹ TiO₂. It was noticed, in particular, that in the most perfect (Ti,Cr)O₂ crystals the hysteresis loop at a given temperature is essentially less distinct than in “bad quality” samples.⁹ Besides, the enormous scatter of effective magnetic moment per cation is observed in all ferromagnetic oxides, and the concentration of magnetic dopants lies far below the percolation threshold x_c associated with the nearest-neighbor cation coupling.⁷ Basing on these facts, one concludes that nonmagnetic defects are also involved in formation of the localized magnetic moments. They influence

their magnitude and localization, and this influence is sensitive to the growth and annealing regimes. In a recent paper¹⁰ the role of shallow exciton states bound with magnetic impurities in ZnO bases compounds is emphasized and the correlation between the experimentally observed chemical trends in ferromagnetism and the electron binding energies to various MIs is stressed.

Recent theories of magnetism in n -type dilute magnetic oxides appeal to magnetic polarons as mediators of indirect exchange between magnetic dopants.^{7,11} In this case the *extrinsic* defects are donor impurities, which donate free electrons occupying the bottom of the conduction band. These electrons form shallow spin-polarized polaronic states due to strong exchange with the localized magnetic moments of transition-metal dopants. A large radius of these states makes the polaronic percolation threshold essentially lower than x_c .

One should note, however, that the free-carrier concentration in these compounds is vanishingly small, and that is why they have been proposed to be called dilute magnetic dielectrics (DMDs).⁸ It means that we need now to find an exchange mechanism, which works in the case of really insulating oxides. In this paper we construct a model of insulating oxide, which considers *intrinsic* nonmagnetic defects as an integral part of the ordering mechanism. We concentrate mainly on the superexchange between magnetic ions mediated by oxygen vacancies, which is believed to be the source of ferromagnetic order in TiO₂ diluted with Co.⁸

II. MODEL OF DILUTE MAGNETIC OXIDE

As has been established three decades ago,^{12,13} the basic microscopic Hamiltonian, which gives an adequate quantitative and qualitative description of electronic and magnetic properties of semiconductors doped by transition-metal ions is the Anderson Hamiltonian¹⁴ (see summarizing monographs^{15,16}). Indirect RKKY,¹⁷ superexchange and double exchange³ interactions between magnetic ions may be derived microscopically from the multisite generalization of the Anderson model.¹⁸ The Hamiltonian of this model reads

$$H = H_h + H_d + H_{hd}, \quad (1)$$

where H_h describes the electronic structure of the host semiconductor, $H_d = \sum_j H_{dj}$ is the Hamiltonian of strongly interacting electrons in the d shells of magnetic ions located in the lattice sites j , and $H_{hd} = \sum_j H_{hdj}$ is the hybridization Hamiltonian describing the covalent bonding between the impurity $3d$ electrons and the host p electrons (the contribution of hybridization with the host s electrons in the effective exchange is generally negligibly small). Usually the direct dp exchange is neglected in the Anderson model, since the indirect exchange coupling dominates in the covalent materials.^{15,16}

From the point of view of the Anderson model, the crucial difference between the narrow-gap and wide-gap semiconductors is in the position of d levels of the impurity electrons relative to the top of the valence band. Due to a strong electron-electron interaction in the $3d$ shell (Coulomb blockade), the impurity energy level ε_d should be defined as an “addition energy” for the reaction $d^{n-1} + e_b \rightarrow d^n$, i.e., the en-

ergy cost $\varepsilon_d - \varepsilon_b$ of adding one more electron, e_b , from the band continuum to the impurity $3d$ shell, where

$$\varepsilon_d = E(d^n) - E(d^{n-1}), \quad (2)$$

$E(d^n)$ is the total energy of a “pseudoion” consisting of an impurity in a configuration $3d^n$ and distorted electron distribution in the host semiconductor, ε_b is the energy of the band electron e_b .^{15,19}

In this definition the energy is counted from the top of the valence band, which is the source of additional electrons for the impurity. It is known, e.g., that Mn, the most popular magnetic impurity, has especially deep d level corresponding to the half filled d shell in the configuration $3d^5$. This level is always occupied in such narrow-band semiconductors as (Ga,Mn)As, (Ga,Mn)P, (In,Mn)As. This means that the addition energy $\varepsilon_d = E(d^5) - E(d^4)$ is well below the energy ε_p of the top of the valence band. On the contrary, $\varepsilon_d > \varepsilon_p$ in the wide gap semiconductors like GaN,²⁰ and the occupation of this state, depends on the type and concentration of other defects.

One should compare this picture with the energy spectra of magnetically doped metal oxides. Situation with the transition-metal impurities in ZnO is apparently close to that in GaN. Both these materials are wide band-gap semiconductors, and the only difference is that the neutral state of magnetic impurity in ZnO is MI^{2+} . The corresponding energy levels arise, as a rule, within the band gap, and the states with other oxidation numbers may appear only due to an additional n or p doping.

The calculation²¹ of addition energies for MI^{n+} states in rutile TiO₂ has shown that the “energy levels” ε_d for neutral MI^{4+} states are usually deep in the valence band for heavy transition-metal ions (starting with Mn), whereas the condition $\varepsilon_d > \varepsilon_p$ is fulfilled for the addition energies of charged MI^{3+} and MI^{2+} ions. Recent LSDA+U calculations²² for anatase TiO₂ doped with Mn, Fe, and Ni are in a general agreement with those earlier cluster calculations.

This means that the ground state of this system should be TiO₂: MI^{4+} . In this situation the Anderson Hamiltonian may be immediately transformed into the sd -exchange model by means of the Schrieffer-Wolff transformation. In the absence of free carriers the short-range effective interimpurity exchange interaction is exponentially weak and there is no chance for magnetic ordering with reasonably high T_C . However, the situation in real materials is quite different. Leaving aside early results for the samples with secondary phase inclusions,⁵ we concentrate on the recent data for the materials, which are believed to be genuine ferromagnetic DMDs free from magnetic precipitates. As was mentioned above, the room-temperature ferromagnetic order was detected in Cr and Co doped anatase TiO₂, and in both cases native defects are involved in formation of the ferromagnetic order.^{8,9} In the latter case these defects are apparently oxygen vacancies. Below, we adapt our theory³ for vacancy mediated indirect exchange. The case of (Ti,Cr)O₂ will be discussed in the concluding section.

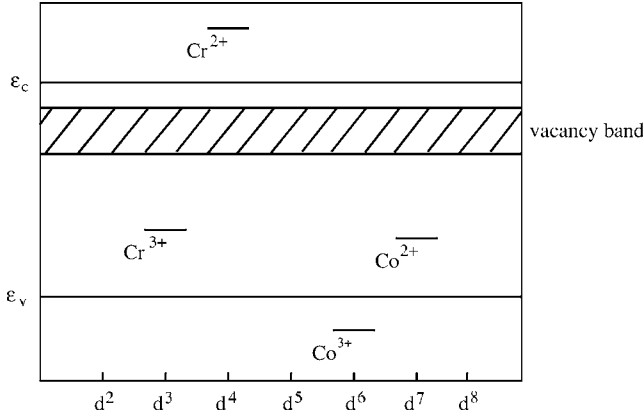
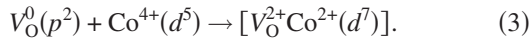


FIG. 1. Impurity-related and vacancy-related energy levels in cation substituted nonstoichiometric TiO_2 .

III. VACANCY-RELATED SUPEREXCHANGE MECHANISM

In the highly insulating ferromagnetic $(\text{Ti},\text{Co})\text{O}_2$, magnetic ions are in Co^{2+} state.⁸ A seeming contradiction with the requirement of electrical neutrality of the substitutional impurities²¹ may be resolved, if one takes into account the intrinsic nonstoichiometry of the samples: oxygen vacancies V_O are created in the process of sample preparation. It follows from the general neutrality consideration that an oxygen vacancy binds two electrons on a discrete level in the band gap to saturate the dangling bonds. In the process of annealing a noticeable amount of oxygen vacancies are captured by Co substitution impurities in cation sites. In the case, when V_O arises in the octahedron containing a Co ion, the double defect Co- V_O is formed, and its stability (or metastability with respect to formation of Ti- V_O complexes) is determined by the charge transfer of these two electrons in accordance with the reaction



A presumable scheme of the energy levels, which substantiates such charge transfer, is shown in Fig. 1. The configurations d^n of $3d$ shells corresponding to different charge states of Co and Cr impurities are pointed out. The dashed band shows the position of vacancy-related levels below the bottom of conduction band ϵ_c .

As a result of charge transfer reaction (3), the vacancy related electrons are captured by $[V_O^{2+}\text{Co}^{2+}]$ complexes, the system remains insulating and the magnetic interaction between these complexes predetermines the magnetic properties of the system.

In this section we construct a microscopic model of impurity-vacancy complexes basing on our previous studies³ of double ferromagnetic exchange in $(\text{Ga},\text{Mn})\text{As}$ and the electronic structure of complexes Cr- V_O in $(\text{Ga},\text{Cr})\text{As}$,²³ as well as on the numerical calculations of the electronic structure of V_O defects in TiO_2 ²⁴ and doped non-stoichiometric (oxygen deficient) $(\text{Ti},\text{Co})\text{O}_2$.^{22,25}

The structure of Hamiltonian, which describes the oxygen deficient $(\text{Ti},\text{Co})\text{O}_2$ is the same as in Eq. (1), but the oxygen vacancies should be taken into account in the host Hamil-

tonian H_h . We start with a quantum-chemical picture of an isolated defect cell, which contains both Co impurity substituting for a Ti cation and the vacancy in one of the apices of oxygen octahedra. We mark the cell by the index j and consider the Hamiltonian

$$H_{vj} = H_{hj}^i + H_{dj} + H_{hdj}. \quad (4)$$

Now the first term H_{hj}^i describes the host crystal with the vacancy V_O in the cell j . This Hamiltonian may be diagonalized, and the resulting spectrum contains the band continuum distorted by the vacancy potential and the discrete levels $\epsilon_{v\mu}$ for electrons bound on the dangling bonds in the defect cell.

The Hamiltonian H_{hdj} rewritten in this basis contains terms describing hybridization with both continuum and discrete states of H_{hj}^i . The general form of H_{hdj} is

$$H_{hdj} = \sum_{\mu\nu\sigma} \sum_{\tau_d\tau_o} [V_{j\nu\mu}(\tau_d, \tau_o) d_{j+\tau_d, \mu\sigma}^\dagger c_{j+\tau_o, \nu\sigma} + \text{H.c.}] + \sum_{\kappa\mu\sigma} \sum_{a=v,c} [V_{ja\mu}(\tau_d, \kappa) d_{j+\tau_d, \mu\sigma}^\dagger c_{\kappa a\sigma} + \text{H.c.}]. \quad (5)$$

Here the operators $d_{j+\tau_d, \mu\sigma}$ and $c_{j+\tau_o, \nu\sigma}$ stand for the localized $d\mu$ and $p\nu$ orbitals on the impurity site $\mathbf{R}_i = \mathbf{R}_j + \tau_d$ and the vacancy site $\mathbf{R}_o = \mathbf{R}_j + \tau_o$, respectively, and the operators $c_{\kappa a\sigma}$ describe the continuous states in the host crystal valence ($a=v$) and conduction ($a=c$) bands.

Information about the vacancy-related states in anatase TiO_2 is rather scanty,²⁶ so we refer to the data available for oxygen-deficient rutile TiO_2 . In accordance with numerical calculations,^{24,25} which correlate with the experimental observations, V_O creates donor levels ϵ_o a few tenths of an eV below the conduction band. The donor electrons saturate the dangling bonds with the neighboring atoms, so that the defect wave function has the largest amplitude at the next Ti neighbor of the vacancy and extends to several coordination spheres. The extended defect states form a band of donor levels already for 1% concentration of oxygen vacancies, i.e., the wave functions of the vacancy states effectively overlap when the vacancies are separated by a distance of about five interatomic spacings. This observation will be used below when estimating the Curie temperature. The calculated electronic structure for Co-doped oxygen deficient anatase TiO_2 gives similar picture for the charge distribution and the density of states.²⁶

This observation verifies the model Hamiltonian (5) for the Co substitutional impurities. Its form implies strong nearest-neighbor hybridization between the vacancy and impurity related states. Since the conduction band of TiO_2 is formed mainly by the d states of Ti sublattice, the matrix elements $V_{c\mu}$ in the second term in this Hamiltonian describe the hybridization of the Co impurity d states with those in the cationic sublattice. Apparently one may neglect the hybridization $V_{c\mu}$ in comparison with $V_{j\nu\mu}$, and retain in this term only the hybridization $V_{j\nu\mu}$ with the oxygen-related p states in the valence band.

We return now to the energy-level scheme Fig. 1 substantiating the charge-transfer reaction (3). It is emphasized that we compare the one-electron energy levels of the oxygen vacancy with the corresponding levels of Co impurities in

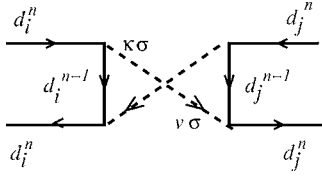


FIG. 2. Diagrammatic representation of the superexchange interaction between two magnetic impurities in charge states d_i^n and d_j^n via the intermediate states d_i^{n-1} and d_j^{n-1} and empty levels $\kappa\sigma$, $\nu\sigma$ (see text for further explanation).

different charge states. These levels are defined as addition energies (2) corresponding to recharging processes $\text{Co}^{m+}/\text{Co}^{(m-1)+}$. These energies may be taken, e.g., from Ref. 21. Hybridization $V_{j\nu\mu}$ allows for an electron transfer of the two electrons from the vacancy level first to the level $\varepsilon_d(3+ / 4+)$ and then to the level $\varepsilon_d(2+ / 3+)$ and formation of the complex defect $[\text{V}_O^{2+}\text{Co}^{2+}]_j$ with seven electrons occupying the 3d-shell of the ion Co^{2+} and empty extended V_O -related states.

Indirect exchange interaction arises when the wave functions of two complexes centered in the cells j and i overlap. It is clear that the overlap is controlled by the radius of extended V_O -related state. An obvious interaction mechanism is the superexchange, where two magnetic impurities exchange electrons via empty vacancy levels. It will be shown below that this interaction favors ferromagnetic ordering in the system.

The simplest way to construct an effective superexchange interaction operator is to project the two-impurity Hamiltonian $\text{H}_{ji} = \text{H}_{dj} + \text{H}_{di} + \text{H}'_{hji} + \text{H}_{hdj} + \text{H}_{hdi}$ onto the subspace $\langle ji | \dots | ji \rangle_{2+}$ with fixed Co^{2+} configurations of the two magnetic ions and also project out the charged impurity states Co^{3+} , which arise due to the hybridization $\text{H}_{hdj} + \text{H}_{hdi}$. Here H'_{hji} is the host Hamiltonian with two oxygen vacancies in the cells j, i . Then the fourth-order term in the impurity-vacancy hybridization

$$\left\langle ji \left| \text{H}_{hdj} \frac{1}{E_0 - \text{H}_{ji}^0} \text{H}_{hdi} \frac{1}{E_0 - \text{H}_{ji}^0} \text{H}_{hdi} \frac{1}{E_0 - \text{H}_{ji}^0} \text{H}_{hdj} \right| ji \right\rangle_{2+} \quad (6)$$

gives the effective exchange vertex, represented graphically in Fig. 2. The resolvents, which appear in Eq. (6) correspond to the ground state E_0 of the nonhybridized Hamiltonian $\text{H}_{ji}^0 = \text{H}_{dj} + \text{H}_{di} + \text{H}'_{hji}$. The solid lines in this diagram stand for the definite charge and spin state of the impurity in the site i or j [$\text{Co}^{2+}(d^7)$ and $\text{Co}^{3+}(d^6)$ in a given spin and orbital configuration]. The vertices correspond to various terms in the hybridization Hamiltonian (5), which changes the impurity state from d_i^7 to d_i^6 and vice versa. In the vertex $V_{\nu\mu}$ an electron appears on the empty vacancy ν orbital with the spin σ . In the vertex $V_{a\mu}$ a hole (electron) appears in the valence (conduction) band. Yet, a similar process $d_j^7 \rightarrow d_j^6 + \nu'\sigma$ occurs around the counterpart site j . Then the two p electrons change their “hosts” (two dashed lines in Fig. 2), and this is the end of the superexchange process. This scheme allows one to roughly estimate the effective exchange coupling as

$$J_Z \sim V^4 / \Delta_{do}^2 D_o, \quad (7)$$

where Δ_{do} is the energy of the transition (3), and D_o is the characteristic energy scale of the vacancy related band under the bottom of conduction band.

A similar estimate may be found, e.g., in Refs. 27, where the superexchange between singly occupied states in the 4f shell via empty states in conduction band was studied (D_o in that case is the conduction-band width). In the case of a singly occupied shell f^1 or d^1 there is no Hund interaction in the unfilled shell. As a result antiferromagnetic part of this interaction prevails (ferromagnetic channels are blocked by the Pauli principle).²⁷ In our case the superexchange mechanism favors the ferromagnetic alignment of spins since the intrashell Hund interaction suppresses the exchange by the electrons with antiparallel spins (see next section).

There seems to be much in common between the vacancy-related mechanism represented by Eqs. (6) and (7) and the spin-polaron mechanism offered in Ref. 7. In both cases the effective radius of magnetic interaction is controlled by the extended donor states. It should be emphasized, however, that unlike the indirect exchange via the states in the donor impurity band,⁷ in our case the occupation of the band of vacancy states is controlled by the difference between the total concentration of oxygen vacancies and the concentration of complex defects $[\text{Co}_{\text{Ti}}, \text{V}_O]$. This mechanism is not related to additional n -type dopants, so that it may be realized in highly insulating materials. On the other hand, the unoccupied states in the band of extended vacancy related states plays, in oxygen deficient (Ti) O_2 , the role similar to that played by the empty states in the hole pockets of p -type (Ga, Mn)As in superexchange between magnetic ions (see Ref. 3). We will return to the comparison of superexchange mechanism in various dilute magnetic compounds in the concluding section.

IV. MICROSCOPIC THEORY OF SUPEREXCHANGE IN DMD

The simple estimate (7) by means of the fourth-order perturbation equation (6) may be essentially improved. Basing on the theory of *isolated* transition-metal impurities in semiconductors,^{15,16} one may consider the effects of single-site hybridization between the d orbitals of impurity and oxygen-related states in the valence band and vacancy levels and then use the perturbation theory approach for the *inter-site* hybridization effects responsible for the superexchange.

It is known that the main result of this hybridization is “swelling” of the wave functions of the impurity d electrons.^{15,16} These functions acquire “tails” formed by a superposition of Bloch waves from valence and conduction bands.²⁸ A localized vacancy state is also a superposition of the same Bloch waves. All these covalent effects modify the simple estimate (7), which necessitates a more refined analysis within the microscopic Anderson-like Hamiltonian.

In this section we will derive equations for the superexchange interaction in the system of defects $[\text{Co}_{\text{Ti}}, \text{V}_O]$ by means of the Green function method developed in Ref. 3. For the purpose of practical calculations within this method,

it is more convenient to write the term H'_{hj} in the model Hamiltonian (4) in the form

$$H'_{hj} = \sum_{\kappa\alpha\sigma} \varepsilon_{\kappa} c_{\kappa\alpha\sigma}^{\dagger} c_{\kappa\alpha\sigma} + \sum_{\nu\sigma} \varepsilon_{\nu\nu} c_{j+\tau_{\nu},\nu\sigma}^{\dagger} c_{j+\tau_{\nu},\nu\sigma}. \quad (8)$$

It is assumed in Eq. (8) that the host Hamiltonian with vacancies has been diagonalized, and the band states are classified by the index κ . Each vacancy in the site $j + \tau_{\nu}$ creates a localized level in the gap. It was found in the previous numerical calculations^{21,24} that both the oxygen-related p states in the valence band and the titanium-related d states from the valence band contribute to formation of localized vacancy states, and the vacancy-related level arises slightly below the bottom of conduction band.

The term H_d describing the subsystem of magnetic impurities in the Hamiltonian (1) has the form

$$H_d = \sum_j H_{dj} = \sum_j \sum_{\mu\sigma} \varepsilon_{\mu} d_{j\mu\sigma}^{\dagger} d_{j\mu\sigma} + H_j^{corr}. \quad (9)$$

Here the site indices are introduced in accordance with the definition given in Eq. (5), H_i^{corr} includes all the Coulomb and exchange interactions responsible for the Hund rule within the $3d$ shells of Co ions. In accordance with this rule the Co d shell contains seven electrons, five of which form the closed “inert” $d_{\uparrow}^5(t_2^3e^2)$ subshell and the remaining two electrons form the open ‘active’ $d_{\downarrow}^2(t_{\mu}e_{\mu'})$ subshell. Only the electrons in the open subshell are involved in the hybridization induced superexchange. The reason for this discrimination is the above-mentioned swelling of the impurity electron wave functions due to the hybridization with the host electrons, which is stronger for the open subshell than for the closed one.^{15,16}

It is easily seen from Eq. (6) that the fourth-order transition

$$\langle d_{j\uparrow}^5 d_{j\downarrow}^2, d_{i\uparrow}^5 d_{i\downarrow}^2 | d_{i\downarrow}^{\dagger} c_{\nu'\downarrow} \mathbf{R}_{ji} d_{j\downarrow}^{\dagger} c_{\nu\downarrow} \mathbf{R}_{ji} c_{\nu\downarrow}^{\dagger} d_{i\downarrow} \mathbf{R}_{ji} c_{\nu\downarrow}^{\dagger} d_{j\downarrow} | d_{j\uparrow}^5 d_{j\downarrow}^2, d_{i\uparrow}^5 d_{i\downarrow}^2 \rangle$$

for the ferromagnetically aligned spins of two impurities is possible. Here $\mathbf{R}_{ji} = (E_0 - H_{ji}^0)^{-1}$ is the zeroth-order resolvent. A similar process

$$\langle d_{j\uparrow}^5 d_{j\downarrow}^2, d_{i\downarrow}^5 d_{i\uparrow}^2 | d_{i\downarrow}^{\dagger} c_{\nu'\downarrow} \mathbf{R}_{ji} d_{j\uparrow}^{\dagger} c_{\nu\uparrow} \mathbf{R}_{ji} c_{\nu\uparrow}^{\dagger} d_{i\uparrow} \mathbf{R}_{ji} c_{\nu\uparrow}^{\dagger} d_{j\downarrow} | d_{j\uparrow}^5 d_{j\downarrow}^2, d_{i\downarrow}^5 d_{i\uparrow}^2 \rangle$$

for the antiferromagnetically aligned spins may either lead to a change of the total orbital momentum of the d shell (occupation of the crystal field split states), then it is suppressed due to the Hund rules for the occupation of subshells, or it may change only the projection of the spin momentum, but then its amplitude is suppressed by the smallness of the corresponding Clebsch-Gordon coefficients. We neglect below the contribution of these processes in the total energy of the system.

Our task now is to calculate the energy lowering due to the electron exchange between the impurities with parallel spin alignment. Since no spin flip occurs in the course of the exchange, the spin index may be omitted in the Hamiltonian (5), (8), (9). This energy gain is given by the following equation:^{3,29}

$$E^{magn} = \frac{1}{\pi} \text{Im} \int_{-\infty}^{\infty} \varepsilon \text{Tr} \Delta \mathbf{G}[\varepsilon - i\delta \text{sgn}(\varepsilon - \eta)] d\varepsilon, \quad (10)$$

where $\Delta \mathbf{G}$ is the part of the single-electron Green function related to the spin-dependent interaction of magnetic impurities,

$$\Delta \mathbf{G}(z) = (z - \mathbf{H})^{-1} - (z - \mathbf{H}'_{hj})^{-1},$$

η is the chemical potential. The integral in Eq. (10) contains contributions from both the valence-band continuum and occupied discrete states in the energy gap.

When calculating $\Delta \mathbf{G}(z)$, we exploited the following features of our problem:

(i) Since we are interested in the energy lowering due to the parallel spin ordering, the spin-flip processes do not contribute to the relevant part of the system of Dyson equations for the Green function and these equations allow for an exact solution.¹⁵

(ii) The calculation procedure may be radically simplified by using the analytical properties of $\text{Tr} \Delta \mathbf{G}(z)$, which allow one to calculate the energy by summing over the empty states instead of integrating over the whole occupied part of the energy spectrum.³

(iii) We are interested only in the trace of the Green function defined in the subspace $\langle d_{\downarrow}^2 d_{\uparrow}^5 | \dots | d_{\downarrow}^2 d_{\uparrow}^5 \rangle$ [see Eq. (6)].

As discussed above, the leading contribution to the formation of complex defect is due to the hybridization between the d shells of magnetic impurities and the unoccupied states in the band of vacancy related states below the bottom of conduction band. Thus our next task is to calculate the upward shift of the V_O -related levels. For this sake one has to find the poles of the single-electron Green function \mathbf{G} . This function has the following block structure:

$$\mathbf{G} = \begin{pmatrix} \mathbf{G}_{\mu\mu'} & \mathbf{G}_{\mu\nu'} & \mathbf{G}_{\mu\nu''} \\ \mathbf{G}_{\nu\mu'} & \mathbf{G}_{\nu\nu'} & 0 \\ \mathbf{G}_{\nu\mu''} & 0 & \mathbf{G}_{\nu\nu''} \end{pmatrix}, \quad (11)$$

where the diagonal blocks are the two impurity ($\mathbf{G}_{\mu\mu'}$), band ($\mathbf{G}_{\nu\nu'}$) and single-vacancy ($\mathbf{G}_{\nu\nu''}$) Green functions, respectively, and the off-diagonal blocks stand for the two types of hybridization. Only valence-band states are taken into account in the band component.

As shown above the exchange energy E^{magn} is given by the shifts of the V_O levels which are determined by the poles of \mathbf{G} . It is sufficient to study the block $\mathbf{G}_{\nu\nu'}$ only since it has the same poles. Moreover, as follows from Eq. (10), in order to calculate its trace we need only its diagonal part $\tilde{\mathbf{G}}_{\nu\nu'}$. It reads

$$\begin{aligned} \tilde{\mathbf{G}}_{\nu\nu'} &= g_{\nu} + g_{\nu}^2 \sum_{i=1,2;\mu} V_{\nu\mu}^*(\mathbf{R}_i) G_{i\mu,i\mu} V_{\nu,\mu}(\mathbf{R}_i) \\ &+ g_{\nu}^2(\varepsilon) \sum_{i,j=1,2;\mu\mu',\nu'} V_{\nu\mu}^*(\mathbf{R}_i) G_{i\mu,i\mu}(\varepsilon) V_{\nu',\mu}(\mathbf{R}_i) g_{\nu'}(\varepsilon) \\ &\times V_{\nu'\mu'}^*(\mathbf{R}_j) G_{j\mu',j\mu'}(\varepsilon) V_{\nu,\mu'}(\mathbf{R}_j). \end{aligned} \quad (12)$$

We have kept the leading terms in the hybridization of the

vacancy and impurity states contributing to the intersite exchange. Hybridization of the empty conduction-band states and the impurity states is neglected in calculation of this exchange [see discussion after Eq. (5) in Sec. III]. Since the spin-flip processes are not involved in the calculation of E^{magn} , the equations may be solved for each spin projection separately, and we omit below the spin index for the sake of brevity.

We represent the impurity Green function in terms of the irreducible representation of the symmetry group of axial defect $[\text{Co}_{\text{Ti}}, \text{V}_\text{O}]$, so that the impurity Green functions are diagonal in this representation

$$G_{i\mu, i\mu} = [\varepsilon - \varepsilon_{i\mu} - \Sigma_{i\mu}(\varepsilon)]^{-1} \quad (13)$$

with the mass operator

$$\Sigma_{i\mu}(\varepsilon) = \sum_{\kappa} V_{\kappa\mu}^*(\mathbf{R}_i) g_{\kappa}(\varepsilon) V_{\kappa\mu}(\mathbf{R}_i) G_{i, i\mu}$$

which results from the exact solution of the corresponding single impurity problem for a given spin.^{13,30,31} Here the index $\kappa = \{v, v'\}$ unites both band and vacancy indices. The bare propagators are defined as

$$g_v = \frac{1}{\varepsilon - \varepsilon_v - i\delta \text{sgn}(\varepsilon - \eta)},$$

$$g_{v'} = \frac{1}{\varepsilon - \varepsilon_{v'} - i\delta \text{sgn}(\varepsilon - \eta)}, \quad g_{i\mu} = \frac{1}{\varepsilon - \varepsilon_{i\mu} - i\delta \text{sgn}(\varepsilon - \eta)}.$$

Using Eqs. (12) and (10) we can find the change of the total energy due to the interaction of the vacancy and impurity states. The second-order correction in the vacancy-impurity hybridization $V_{\mu, v}(\mathbf{R}_i)$ in Eq. (12) is a single impurity effect and has nothing to do with the exchange interaction. The latter appears only in the last term of Eq. (12), which is of the fourth order. It describes a shift of the vacancy levels due to the electron exchange between the two impurities, *which is possible only provided the spins of two impurities are parallel*.

The upward shift of the empty vacancy levels corresponds to lowering of the total energy of the system [see discussion after Eq. (10) and in Appendix of Ref. 3]. Hence we come to the equation for the kinematic exchange (superexchange) energy between the two magnetic impurities,

$$E_{ij}^{magn} = -2 \sum_{v, \mu, \mu'} \frac{V_{v\mu}^*(\mathbf{R}_i) V_{v, \mu'}(\mathbf{R}_j) P_{ij, \mu\mu'}(\varepsilon_v)}{[\varepsilon_v - \varepsilon_{i\mu} - P_{i\mu}(\varepsilon_v)][\varepsilon_v - \varepsilon_{j\mu'} - P_{j\mu'}(\varepsilon_v)]}, \quad (14)$$

where $P_{ii\mu}(\varepsilon) = \text{Re} \Sigma_{i\mu}(\varepsilon)$. Here

$$P_{ij, \mu\mu'}(\varepsilon_v) = \sum_{v' \neq v} \frac{V_{v'\mu}(\mathbf{R}_i) V_{v', \mu'}^*(\mathbf{R}_j)}{\varepsilon_v - \varepsilon_{v'}} \quad (15)$$

is an analog of the standard lattice Green function defined on the states of irregular vacancy ‘‘lattice’’ and weighted with the hybridization matrix elements. The summation over v' is carried out over all the states of the vacancy band, whereas the summation over v is carried out only over the free states

in the vacancy band, i.e., $\varepsilon_{v'} > \eta$. Equation (14) has a structure similar to that of Eq. (10) of Ref. 3. The role of hole pockets is now played by the unoccupied vacancy states, and the fact that there is no free carriers and, hence no Fermi surface, so important for the RKKY model, plays now no role whatsoever. Besides, contrary to the polaronic model,⁷ the ferromagnetism with high enough T_C arises in our model without additional enhancement due to spin polarization of the vacancy related band (see more detailed discussion below).

The fourth-order exchange energy can be interpreted by means of the diagram presented in Fig. 2. Now the dashed lines in this diagram correspond to the two vacancy states virtually occupied in the superexchange act. Two multipliers in the denominator in Eq. (14) are the energies $\tilde{\Delta}_{d_o, i}$ required for the two ‘‘reactions’’ $\text{Co}(d^7) \rightarrow \text{Co}(d^6) + \text{V}_\text{O}(p)$ in the sites i, j . These energies, include also the ligand field shifts $P_{d: i\mu}$ of the impurity d levels.^{12,13,29} The summation over unoccupied states v' gives a contribution of the order of the vacancy band width D_o due to the factor $(\varepsilon_v - \varepsilon_{v'})$, in the denominator of Eq. (15). Thus the calculation of exchange energy by the Green function method by means of Eqs. (10) and (14) confirms the qualitative estimate (7).

Now we are in a position to derive the effective spin Hamiltonian for interacting magnetic defects. Since we integrated out all the charge degrees of freedom when calculating the energy E_{ij}^{magn} , this Hamiltonian has the simple form

$$H_{ex}^{eff} = \frac{1}{2} \sum_{\langle ij \rangle} J_{\langle ij \rangle} \mathbf{S}_i \mathbf{S}_j, \quad (16)$$

where \mathbf{S}_i is the spin of the ion $\text{Co}(d^7)$, and the exchange constant $J_{\langle ij \rangle}$ is determined as the energy difference *per bond* between the parallel and antiparallel orientations of spins in the pair $\langle ij \rangle$. One may identify the coupling constants as $2J_{\langle ij \rangle} S(S+1) = E_{ij}^{magn}$. Since these coupling constants are negative, they lead to a ferromagnetic ordering at temperatures below the Curie temperature T_C . Well beyond the percolation threshold (which may be identified with the minimal vacancy concentration sufficient for formation of the vacancy band) T_C may be estimated as

$$T_C = \frac{1}{k_B} \frac{zS(S+1)}{3} |J| = \frac{z}{6k_B} |E^{magn}|. \quad (17)$$

Here $|E^{magn}|$, and respectively $|J|$, is the typical value of the superexchange interaction in the pair of impurities separated by a distance not exceeding the double localization radius R_o of the vacancy state, z is the number of Co impurities within the corresponding volume. As was mentioned above the fact that 1% of vacancies is sufficient for formation of a band, means that the typical distance between them is smaller than $2R_o$. Since nearly each Co atom forms a complex with an oxygen vacancy, a 2% concentration of Co atoms substitutions means a 1% vacancy concentration when the vacancy states form a band. This fact guaranties that each Co atom interacts not only with its own vacancy but also with other neighboring vacancies, which form pairs with other Co atoms.

Magnetic ordering with a high T_C in (Ti,Co)O₂ is observed at higher Co concentrations up to 6% which correspond to the concentration of vacancies captured by the Co impurities $\sim 3\%$. Since the band in the forbidden energy gap is formed at 1% concentration of vacancies, one may expect that the coordination number for such a concentration may be at least 3–4. At a three times higher concentration the coordination number will certainly become larger and a rough estimate $z \approx 10$ seems to be quite reasonable. We do not have in our disposition precise experimental data concerning positions of the V_O level in anatase TiO₂, so we refer the data available for the rutile modification where the donor levels related to an isolated V_O are found at a few tenth of 1 eV below the bottom of conduction band.²⁴ Using for the forbidden band width the experimental value 3.2 eV and basing on the calculations of Co-related d -level positions in the forbidden energy gap presented in Ref. 22, one may estimate the pd charge-transfer gap $\tilde{\Delta}_{pd} \sim 1$ eV. The width of the vacancy band D_o as well as the magnitude of hybridization parameter strongly depend on the specific characteristics of the sample (vacancy concentration, annealing regime, etc.). Besides, the vacancy band may or may not be partially filled due to uncontrollable donor impurities. Taking for an estimate the average value of $V_{\nu\mu} \sim 0.1$ eV, assuming the same estimate for D_o , and substituting the value of $S=3/2$ into Eq. (17) one gets $T_C \sim \gamma z 10^{-4}$ eV $\approx \gamma 100$ K for $z=10$. The coefficient γ includes all the uncertainties (degeneracy factor of vacancy and impurity levels, difference between the intracell and intercell hybridization parameters, uncertainties in the effective coordination number z , etc. We expect the factor γ to be ideally close to 1. However, it may deviate, and even strongly, from this value depending on the preparation history of each particular sample. Unfortunately, it is rather difficult to find optimal conditions for high T_C in such a multi-factor situation.

One may calculate, however, the variation of the Curie temperature as a function of the vacancy band occupation by means of Eqs. (17) and (14). According to the general theory of impurity bands,³² the density of localized states $\rho(\varepsilon)$ below the bottom of conduction band is a complicated function of concentration, which may possess some dips around the positions of isolated vacancy levels (at least at not very high concentration of defects). To demonstrate the general trends, we model $\rho(\varepsilon)$ by means of the sum $\rho(\varepsilon) = \rho_-(\varepsilon) + \rho_+(\varepsilon)$ of two Gaussians

$$\rho_{\pm}(\varepsilon) = \frac{1}{4} \sqrt{\frac{2}{\pi}} \exp\left\{-\frac{(\varepsilon \pm \Delta)^2}{\sigma^2}\right\}$$

shifted by Δ with respect to the center of the band. The density of states may have a dip around $\varepsilon=0$ at large enough Δ . This approximation does not take into account the possible asymmetry of $\rho(\varepsilon)$. Besides, we neglect the energy dependence of the hybridization matrix elements, which may be significant for the states in the “tails” of impurity band beyond the mobility edges.

The dependence of T_C on the band occupation (controlled by the chemical potential η) is presented in Fig. 3 for the cases of $\rho(\varepsilon)$ with and without a dip, respectively. The kin-

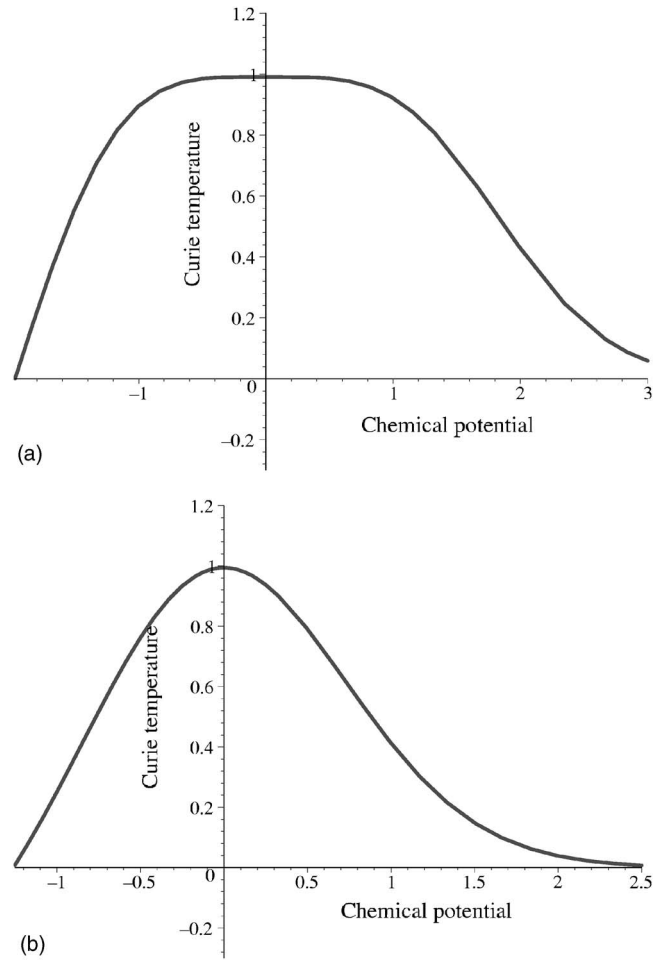


FIG. 3. Dependence of T_C on the vacancy band occupation in accordance with Eqs. (17) and (14). The density of states is modeled by the sum of two shifted Gaussians, $\rho(\varepsilon) = \rho_-(\varepsilon) + \rho_+(\varepsilon)$ for $\Delta/\sigma=2.2$ (a) and $\Delta/\sigma=0$ (b). The zero energy, i.e., the middle of the band, corresponds to the position of the isolated vacancy level. The chemical potential is plotted in the dimensionless units η/σ with $\sigma=2$, $T_C(\eta)$ is normalized by $T_C(0)$, the position of the impurity resonance level is taken at $\varepsilon_i/\sigma=-10$.

ematic exchange is ineffective if the vacancy band is completely empty [the Green function (15) is negative at the energies $\varepsilon_{\nu'} < 0$] or completely occupied (no free states for the exchange process). The ferromagnetic order is stabilized at finite albeit small occupation of the band and the maximal T_C is achieved for the half filled band.

We are not aware of detailed studies of the influence of the occupation of (Ti,Co)O₂ vacancy band on the magnitude of T_C , but there is evidence in favor of this effect in other materials of the DMD family, namely the oxygen-deficient (Zn,Co)O and (Zn,Mn)O.³³ In this paper the room-temperature magnetization was measured as a function of the carrier density at donor levels. The results presented in Fig. 6 of that paper are strikingly similar to the curve presented in Fig. 3(b). Since the magnetization at a given T follows the variation of T_C with the carrier concentration, such similarity seems encouraging for our model. Another related result was obtained in the system (Ga,Mn)N.³⁴ In that material the impurity band in the gap is formed by substitutional Mn,^{3,35} and

codoping $\text{Ga}_{1-x}\text{Mn}_x\text{N}$ epilayers by silicon results in a complete suppression of ferromagnetism, which corresponds to a complete occupation of the impurity band.

V. CONCLUDING REMARKS

Among many dilute magnetic dielectrics only one example has been chosen, namely oxygen deficient $(\text{Ti},\text{Co})\text{O}_2$, and it has been shown that the imperfection of this crystal is crucially important for the formation of a long-range magnetic order. This idea is supported by the recent experimental observation: ferromagnetism is suppressed in Co doped TiO_2 film with high structural quality.⁹ Similar correlations between the quality of films and the magnetism were discovered in Ref. 9 for $(\text{Ti},\text{Cr})\text{O}_2$. It follows directly from our theory that without additional defects creating shallow levels under the bottom of conduction band, the radius of magnetic correlation is too short to overcome the percolation threshold, so that improvement of the film quality is detrimental for magnetic ordering in DMD.

It is also noticed in Ref. 9 that the charge state of chromium impurities in TiO_2 is Cr^{3+} . This fact is easily understood within the framework of our hypothesis about the origin of magnetic order in DMDs. Indeed, the difference between Co and Cr from the point of view of their electronic levels in host TiO_2 [in fact, the addition energies defined in Eq. (2) for the two impurities] is the position of these levels relative to the shallow defect levels. In correlation with the experimental data on electron spin resonance signal and theoretical calculations of the addition energies,²¹ the level of Cr^{2+} state in rutile TiO_2 is higher than the levels of shallow impurities and apparently higher than the bottom of conduction band. We assume that the situation is similar in anatase TiO_2 , so that the same charge-transfer mechanism, which

binds the ions Co^{2+} with oxygen vacancies, should stabilize chromium impurities in a state Cr^{3+} (see Fig. 1),



It is worth also mentioning that generally we may expect that the chemical trends in the Curie temperature for various transition-metal impurities should correlate with the deep level energies (see, e.g., Ref. 10).

Another experimental fact, which requires a theoretical explanation, is a strong sample dependent scatter of saturation magnetic moment M_s , which also depends on the fabrication conditions.^{7,9} This fact may be easily explained if one recognizes that only part of oxygen vacancies is bound to magnetic impurities. “Free” vacancies, V_{O} retain their electrons and eventually donate them to the vacancy band. The partially occupied band is spin polarized, and this polarization may enhance or partially compensate the magnetization of transition-metal ions depending on the net sign of effective exchange in this band.^{7,25,26}

To conclude, we have proposed in this paper a mechanism of ferromagnetic exchange in dielectric nonstoichiometric TiO_2 doped with transition-metal impurities, which involves the interaction between magnetic ions and oxygen vacancies and proposed a qualitative explanation of the basic properties of these materials. A quantitative calculations of electronic structure of magnetically doped TiO_2 based on the model described in this paper will be presented in forthcoming publications.

ACKNOWLEDGMENTS

The authors are indebted to D. Khomskii, K. Krishnan, A. Pakhomov, and T. Ziman for valuable comments. We are thankful to T. Smith who has drawn our attention to Ref. 33.

*Email address: fleurov@post.tau.ac.il

¹*Semiconductor Spintronics and Quantum Computation*, edited by D. D. Awschalom, D. Loss, and N. Samarth (Springer, Berlin, 2002).

²T. Dietl, H. Ohno, F. Matsukura, J. Cibert, and D. Ferrand, *Science* **287**, 139 (1998); T. Jungwirth, W. A. Atkinson, B. H. Lee, and A. H. MacDonald, *Phys. Rev. B* **59**, 9818 (1999); T. Dietl, H. Ohno, and F. Matsukura, *ibid.* **63**, 195205 (2001).

³P. M. Krstajić, V. A. Ivanov, F. M. Peeters, V. Fleurov, and K. Kikoin, *Europhys. Lett.* **61**, 235 (2003); P. M. Krstajić, F. M. Peeters, V. A. Ivanov, V. Fleurov, and K. Kikoin, *Phys. Rev. B* **70**, 195215 (2004).

⁴R. Bouzerar, G. Bouzerar, and T. Ziman, *Phys. Rev. B* **73**, 024411 (2006).

⁵S. J. Pearton, W. H. Heo, M. Ivill, D. P. Norton, and T. Steiner, *Semicond. Sci. Technol.* **19**, R59 (2004).

⁶C. Zener, *Phys. Rev.* **82**, 403 (1951).

⁷J. M. D. Coey, M. Venkatesan, and C. B. Fitzgerald, *Nat. Mater.* **4**, 173 (2005).

⁸K. A. Griffin, A. B. Pakhomov, C. M. Wang, S. M. Heald, and K. M. Krishnan, *J. Appl. Phys.* **97**, 10D320 (2005); *Phys. Rev.*

Lett. **94**, 157204 (2005).

⁹T. C. Kaspar, S. M. Heald, C. M. Wang, J. D. Bryan, T. Droubay, V. Shutthanandan, S. Thevuthasan, D. E. McCready, A. J. Kellock, D. R. Gamelin, and S. A. Chambers, *Phys. Rev. Lett.* **95**, 217203 (2005).

¹⁰K. R. Kittilstved, V. K. Liu, and D. R. Gamelin, *Nat. Mater.* **5**, 291 (2006).

¹¹D. E. Angelescu and R. N. Bhatt, *Phys. Rev. B* **65**, 075211 (2002); A. C. Durst, R. N. Bhatt, and P. A. Wolff, *ibid.* **65**, 235205 (2002).

¹²F. D. M. Haldane and P. W. Anderson, *Phys. Rev. B* **13**, 2553 (1976).

¹³V. N. Fleurov and K. A. Kikoin, *J. Phys. C* **9**, 1673 (1976).

¹⁴P. W. Anderson, *Phys. Rev.* **124**, 41 (1961).

¹⁵K. A. Kikoin and V. N. Fleurov, *Transition Metal Impurities in Semiconductors* (World Scientific, Singapore, 1994).

¹⁶A. Zunger, in *Solid State Physics*, edited by H. Ehrenreich and D. Turnbull (Academic, Orlando, 1986), Vol. 39, p. 276.

¹⁷C. Timm and A. H. MacDonald, *Phys. Rev. B* **71**, 155206 (2005).

¹⁸S. Alexander and P. W. Anderson, *Phys. Rev.* **133**, A1594 (1964).

¹⁹J. W. Allen, *Proceedings of the 7th International Conference on*

- Physics and Semiconductors* Dunod, Paris, 1964, p. 261; J. M. Noras and J. W. Allen, *J. Phys. C* **13**, 3511 (1980).
- ²⁰P. Mahadevan and A. Zunger, *Phys. Rev. B* **69**, 115211 (2004); K. Sato, P. H. Dederichs, H. Katayama-Yoshida, and L. Kudrnovsky, *J. Phys.: Condens. Matter* **16**, S5491 (2004).
- ²¹K. Mizushima, M. Tanaka, and S. Iida, *J. Phys. Soc. Jpn.* **32**, 1519 (1972); K. Mizushima, M. Tanaka, A. Asai, S. Iida, and J. B. Goudenough, *J. Phys. Chem. Solids* **40**, 1129 (1979).
- ²²M. S. Park, S. K. Kwon, and B. I. Min, *Phys. Rev. B* **65**, 161201(R) (2002).
- ²³K. Kikoin, P. Lyuk, L. Pervova, and R. Vanem, *J. Phys. C* **19**, 4561 (1986).
- ²⁴J. W. Halley and H. B. Shore, *Phys. Rev. B* **36**, 6640 (1987).
- ²⁵V. I. Anisimov, M. A. Korotin, I. A. Nekrasov, A. S. Mylnikova, A. V. Lukoyanov, J. L. Wang, and Z. Zeng, *J. Phys.: Condens. Matter* **18**, 1695 (2006).
- ²⁶H. Weng, X. Yang, J. Dong, H. Mizuseki, M. Kawasaki, and Y. Kawazoe, *Phys. Rev. B* **69**, 125219 (2004).
- ²⁷A. N. Kocharyan and D. I. Khomskii, *Fiz. Tverd. Tela (Leningrad)* **17**, 462 (1975) [*Sov. Phys. Solid State* **17**, 290 (1975)]; A. N. Kocharyan and P. S. Ovnanyan, *Zh. Eksp. Teor. Fiz.* **74**, 620 (1978) [*Sov. Phys. JETP* **47**, 326 (1975)].
- ²⁸These Bloch tails are responsible for the Co-3d related peaks in the density of states near the top of the valence band on $\text{Ti}_{1-x}\text{Co}_x\text{O}_2$ in the band calculations of Ref. 22.
- ²⁹B. Caroli, *J. Phys. Chem. Solids* **28**, 1427 (1967).
- ³⁰K. A. Kikoin and V. N. Fleurov, *J. Phys. C* **10**, 4295 (1977).
- ³¹E. N. Economou, *Green's Functions in Quantum Physics*, (Springer, Berlin, 1983) Chap. 5.
- ³²I. M. Lifshitz, S. A. Gredeskul, and L. A. Pastur, *Introduction to the Theory of Disordered Systems* (Wiley, New York, 1988).
- ³³X. H. Xu, H. J. Blythe, M. Ziese, A. J. Behan, J. R. Neal, A. Mokhtari, R. M. Ibrahim, A. M. Fox, and G. A. Gehring, *New J. Phys.* **8**, 135 (2006).
- ³⁴M. Strassburg, M. H. Kane, A. Asghar, Q. Song, Z. J. Zhang, J. Senawiratne, M. Alevi, N. Dietz, C. J. Summers, and I. T. Ferguson, *J. Phys.: Condens. Matter* **18**, 2615 (2006).
- ³⁵K. Sato, P. H. Dederichs, and H. Katayama-Yoshida, *Europhys. Lett.* **61**, 403 (2003).